Application of Spectral Estimation to Laser Doppler Velocimetry and Sizemetry

Th. Wriedt, K. Bauckhage, A. Schöne

University of Bremen, FB 4, P.O. Box 330 440, 2800 Bremen 33, FRG

RESUME

L'analyse des signaux dans le domaine des fréquences a été appliquée à la vélocimétrie Laser Doppler et à la granulométrie (LDVS) pour maîtriser les problèmes posés par le bruit de fond pour détecter et compter les passages au zéro du signal Doppler. Un nouveau processeur LDVS a été développé pour l'application aux jets de métaux fondus atomisés. Dans ce cas, le bruit de fond représente un problème important. La solidification rapide du métal fondu conduit à une surface des particules rugueuse qui réduit le rapport signal-bruit de fond du signal Doppler. La forte concentration de particules ou l'encrassement de la fenêtre d'observation peuvent être d'autres sources de bruits. Le processeur de signaux LDVS proposé a été testé avec des signaux Doppler parasités générés artificiellement qui ont été également analysés dans le domaine des temps avec un "zero crosser". Les mesures experimentales ont donné les variances de l'estimation des fréquences et des différences de phases qui ont été comparées à la limite Cramér-Rao inférieure de la variance. Le nouveau processeur LDVS a également été testé avec des particules de métaux rugueuses dont la distribution de taille a été comparée à celle obtenue par tamisage.

SUMMARY

Analysis of signals in the spectral domain has been applied to Laser Doppler velocimetry and sizemetry (LDVS) to overcome the problems encountered with common counter-type processing of noisy Doppler signals. A new LDVS processor has been developed for application to spray atomisation of molten metals. In this application noise is especially a problem. Rapid solidification of molten metal results in a rough particle surface, which will decrease the signal-to-noise ratio of the detected burst signals. Other noise sources may be a high particle concentration or dirty process windows. The proposed LDVS signal processor has been evaluated by analysing artificially generated noisy burst signals both by this processor and by a counter-type processor. From the measurement results the variances of the frequency and the phase difference estimator have been obtained and compared to the Cramér-Rao lower bound of the variance. The new LDVS processor has also been tested with a set of rough metal particles and the particle size distribution is compared to a distribution measured by sieving.

Introduction

Laser Doppler Velocimetry and Sizemetry (LDVS) is finding widespread application in multiphase flows. By this method the size and the velocity of spherical particles may be measured non-intrusively to describe the process by velocity and size distributions and to compute energy and mass balances [1]. With LDVS two coherent laser beams aimed at the same point within a spray cone produce a set of interference fringes as is shown in Figure 1. The reflections of the fringes are detected by two photomultipliers situated at different angular positions. The frequency of the burst-like signals detected corresponds to the velocity of the particle and the difference in phase of the two burst signals detected simultaneously corresponds to the diameter of the particle. The burst signals are commonly analysed by counter processors which prove to be reliable at high signal-to-noise ratios (SNR). At low signal-to-noise ratios many signals will be discarded by the validation scheme of the counter processor. Noise is especially a problem in investigating spray atomisation of metal which is a new technology to produce semi-finished products [2]. Shrinking effects of the metal particle surface under rapid quenching conditions give rise to rough surface structures which result in diffuse reflections and therefore in noisy signals. To cope with noisy burst signals different spectral estimation schemes have been proposed. Some of the processors based on the Fourier transform are already on the market and others are just approaching the market [3, 4]. Parametric spectral estimation has been proposed [5] but a real time implementation of such a system will hardly be possible in the next years.

LDVS-Fourier transform processor

The block diagram of the LDVS Fourier transform processor we designed is shown in Fig. 2 [6]. The LDVS Fourier transform processor is based on a TMS320C25 plug-in card fitted into an AT-computer. This card was chosen because it is one of a range of signal processing plug-in cards equipped with a standardised digital expansion bus [7]. The TMS320C25 digital signal processor chip was favoured because the Texas Instruments TMS 320 digital signal processor series is the most common one and common algorithms like FFT are available [8]. The processing algorithm consists of a fast Fourier transform (FFT) algorithm followed a search routine which is looking for the maximum line of both calculated spectral densities. The complex amplitude of the maximum spectral line and the two lines nearly are used to calculate the frequency and the phase of the signals [9].

Zero crossing detection

Zero crossing counting or equivalently counting the numbers of extrema in the time signal is widely used to determine the frequency and the phase difference of LDVS burst signals. This signal analysis technique is simple and faster than other more sophisticated methods. It gives good estimates of frequency and phase difference of signals having a signal-to-noise ratio as low as 10 dB. With our system the signals are digitised by an Analog Devices transient recorder and are then transferred to an AT-computer. On the AT-computer an algorithm looking for extrema in the digitised time signals is implemented. The algorithm is based on a two level crossing scheme which ensures that local extrema caused by noise peaks are discarded.

Simulation results

The highpass filtered burst signal can be described by an sinusoid with a Gaussian envelope and a noise component:

$$x_k = e^{-2(k\,\Delta t - T_B)^2/\sigma_B^2}\ \sin(2\pi f\,\Delta t) + w_k$$

$$\sigma_B = \frac{0{,}5\,N_B}{f}$$

$$T_B = -\sigma_B$$

Half the duration of the burst is given by T_B corresponding to an amplitude of the burst which is e^{-2} of the maximum value. t is the sampling interval, N_B the number of periods in the burst, f the frequency and w_k the noise component. The second burst can be described by the same formula apart from a time lag representing the phase shift.

To generate artificial burst signals this formulas have been implemented on an Analog Devices waveform generator. Hundred burst signals having the same signal-to-noise ratio have been generated and processed both by the Fourier transform processor and by the extrema detection system. The bursts generated had a frequency of 1250 kHz. The phase difference was 45 degrees and the

noise signal had a bandwidth of 2 MHz. The number of periods in the bursts was 40. With the Fourier transform processor the sampling frequency was 4 MHz and 128 sampling points were processed. With the extrema detection system the sampling frequency was 50 MHz and 1024 sampling points were processed. Because the Fourier transform algorithm may be interpreted as a maximum likelyhood estimator of frequency and phase the Cramér-Rao lower bound of the variance may be used as a performance standard [10]. In Figure 3 the standard deviation of the frequency estimator calculated from the measurement results is plotted together with the Cramér-Rao lower bound. The standard deviation of the Fourier transform system compares very good with the lower bound. The standard deviation of the estimator based on extrema detection is not as good. In the next Figure 4 the mean frequency estimate is given. The Fourier transform result show less bias than the results measured with the extrema detection system. In estimating the phase difference the Fourier transform system also proves to give better results than the counter-type system as is seen from Figure 5. In the Figure 6 the mean phase difference estimates, obtained by the Fourier processor and the counter-type system are plotted. The results of the Fourier processor show practically no bias.

Measurement results

To show the performance of the LDVS Fourier transform processor it was tested with a set of rough tin-bronze particles. The particles had been generated by metal spraying. The size of these particles could not be measured by LDVS and a counter processor because they generated burst signals having a signal-to-noise ratio of about 0 dB. The size fraction 160-200 µm investigated was obtained by sieving. A quantity of 7 g was continuously circulated by compressed air through the measuring volume. In Figure 7 the particle size distributions given as cumulative number distributions measured by the LDVS FFT method and from by sieving are given. Because only burst signals which lead to the same measured frequency in both chanals where considered valid only about ten percent of all detected particles could be analysed by the Fourier transform method. The average size is the same in both distributions but the size distribution measured by the LDVS FFT method is much broader than the distribution obtained by sieving. This may be explained with the low signal-to-noise ratio of the signals as the simulation results show. The size fraction obtained by sieving may also contain non-spherical particles and this in general leads to broader LDVS distributions because an equivalent diameter based on the measured radius of curvature is measured. Other explanations are deformation of particles caused by the recirculation apparatus or additional small particles generated by abrasion.

Conclusion

A Fourier transform based LDVS signal processor has been described for application to burst signals corrupted by noise. The instrument was tested with artificially generated noisy burst signals. The measurement results are better than results obtained by a counter-type system. The performance of the processor was demonstrated by measuring the size distribution of rough tin-bronze particles which could not be analysed by a counter processor.

Literature

[1] K. Bauckhage, "The Phase-Doppler-Difference-Method, a New Laser-Doppler Technique for Simultaneous Size and Velocity Measurement," Part 1, Part. Part. Syst. Charact. vol. 5, pp.16-22, March 1988.

[2] R.W. Evans, A.G. Leathan and R.G. Brooks, "The Ospray Preform Process," Powder Metallurgy, vol. 28, no. 1, pp. 13-20, 1985.

[3] L. Lading, "Spectrum analysis of LDA signals," in Proc. of an Int. Specialists Meeting on 'The Use of Computers in Laser Velocimetry', Saint-Louis, pp. 20.1-13, May 18-20, 1987.

[4] D. Modarress, H. Tan, A. Nakayama, "Evaluation signal processing technique in Laser anemometry", in Proc. Fourth Intern. Symp. on Applications of Laser Anemometry to Fluid Mechanics, pp. 1.20.1-6, 1988.

[5] C.-V. Venter, P.L. Swart, "A versatile signal processor for Laser-Doppler anemometry," in Proc. Fourth Intern. Symp. on Applications of Laser Anemometry to Fluid Mechanics, pp. 3.20.1.-4, 1988.

[6] K. Bauckhage, A. Schöne, Th. Wriedt, "Using Fast-Fourier-Transform (FFT) for the Phase-Doppler-Difference-Analysis of Powder Metal Sprays," presented at Int. Conf. Laser Technologies in Industry, Porto, Portugal, 6-8 June, 1988.

[7] A. Kohl, "PC-gestütztes Entwicklungs- und Anwendungssystem für digitale Signalprozessoren", Elektronik, vol.37, no.19, pp.132-137, 1988.

[8] P. Papamichalis, J. So, "Implementation of Fast Fourier Transform Algorithms with the TMS32020," in Digital Signal Processing Applications with the TMS320 Family, Houston, TX: Texas

Instruments Inc., 1986.
[9] R.D. Rajaona, P. Sulmont, "A Method of Spectral Analysis Applied to Periodic and Pseudoperiodic Signals," J. of Computational Physics, vol.61, pp.186-193, 1985.
[10] D.R. Rife, R.R.Boorstyn, "Single-Tone Parameter Estimation from Discrete-Time Observations," IEEE Trans. Inform. Theory, vol.IT-20, pp.591-598, Sept. 1977.

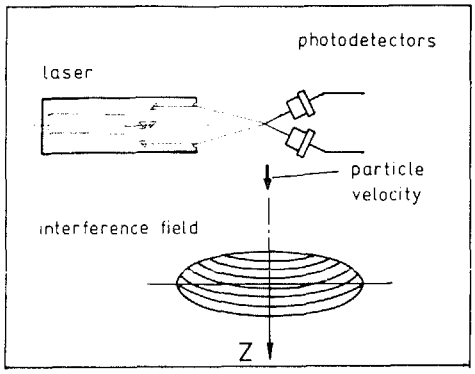

Figure 1. Schematic of the LDVS-method.

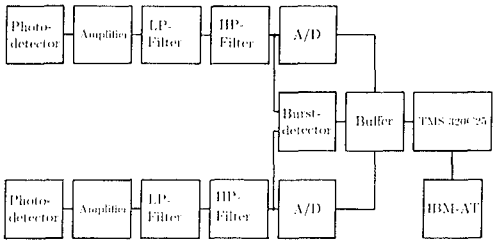

Figure 2. Block diagram of LDVS Fourier transform processor.

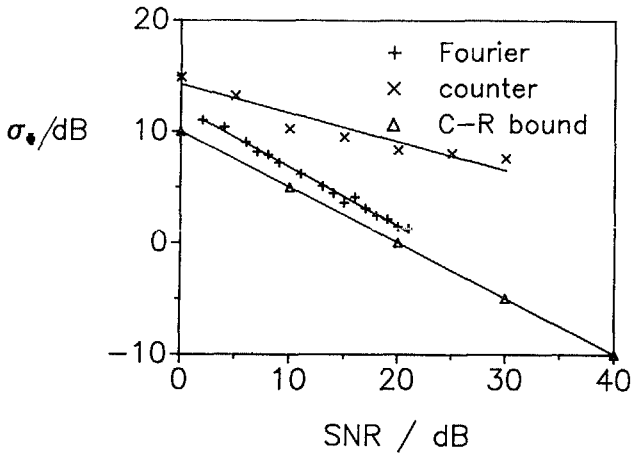

Figure 5. Standard deviation of the phase estimator.

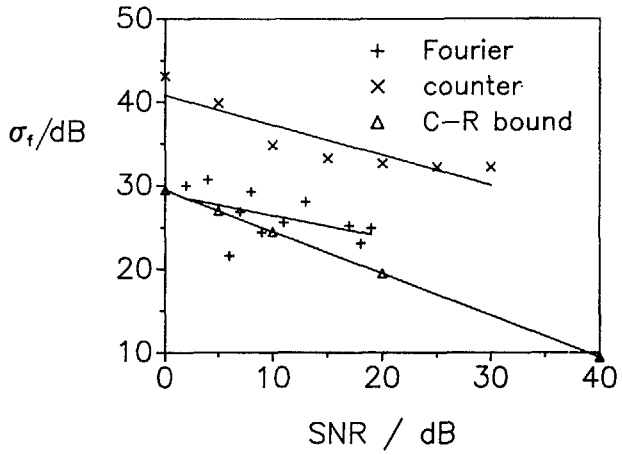

Figure 3. Standard deviation of the frequency estimator.

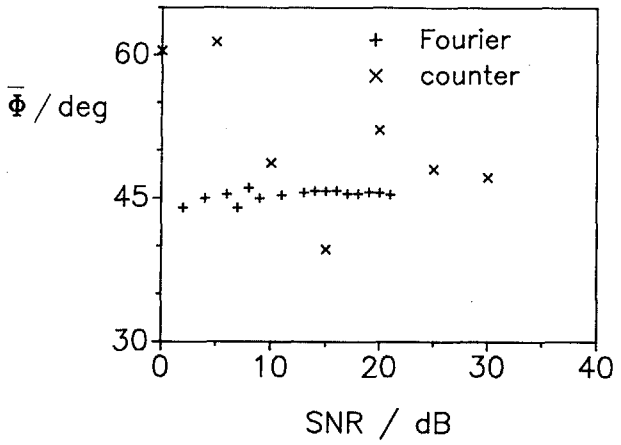

Figure 6. Mean value of the phase estimator.

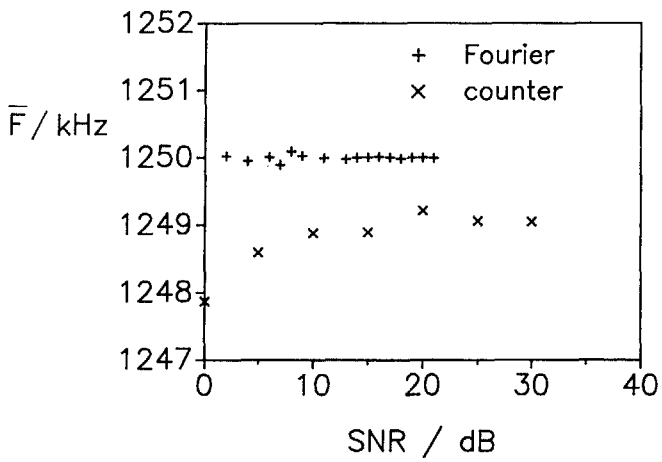

Figure 4. Mean value of the frequency estimator.

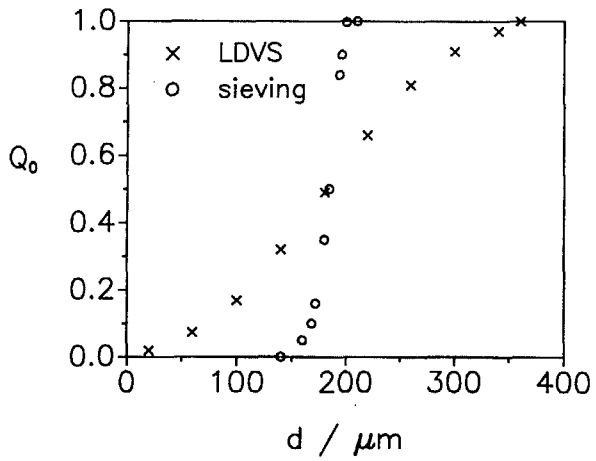

Figure 7. Cumulative particle size distribution.